J|A|C|S
ARTICLES
Published on Web 01/24/2006

Functionalized Gold Nanoparticles as Phosphorescent Nanomaterials and Sensors

Binil Itty Ipe, Karuvath Yoosaf, and Kakkudiyil George Thomas*

Contribution from Photosciences and Photonics, Regional Research Laboratory (CSIR), Trivandrum 695 019, India

Received June 30, 2005; E-mail: georgetk@md3.vsnl.net.in

Abstract: Ligand-capped gold nanoparticles were synthesized by capping monothiol derivatives of 2,2′-dipyridyl onto the surface of Au nanoparticles (Au−BT). The average size of the metal core is around 4 nm, with a shell of ∼340 bipyridine ligands around the Au nanoparticle. The high local concentration of the chelating ligands (∼5 M) around the Au nanoparticle makes these particles excellent ion sponges, and their complexation with Eu^{III}/Tb^{III} ions yields phosphorescent nanomaterials. Absorption spectral studies confirm a 1:3 complexation between Eu^{III}/Tb^{III} ions and bipyridines, functionalized on the surface of Au nanoparticles. The red-emitting Au−BT:Eu^{III} complex exhibits a long lifetime of 0.36 ms with six line-like emission peaks, whereas the green-emitting Au−BT:Tb^{III} complex exhibits a lifetime of 0.7 ms with four line-like emission peaks. These phosphorescent nanomaterials, designed by linking BT:Eu^{III} complexes to Au nanoparticles, were further utilized as sensors for metal cations. A dramatic decrease in the luminescence was observed upon addition of alkaline earth metal ions (Ca^{2+}, Mg^{2+}) and transition metal ions (Cu^{2+}, Zn^{2+}, Ni^{2+}), resulting from an isomorphous substitution of Eu^{III} ions, whereas the luminescence intensity was not influenced by the addition of Na^{+} and K^{+} ions. Direct interaction of bipyridine-capped Au nanoparticles with Cu^{2+} ions brings the nanohybrid systems closer, leading to the formation of three-dimensional superstructures. Strong interparticle plasmon interactions were observed in these closely spaced Au nanoparticles.

Introduction

Rational design of functional nanomaterials is of current interest because of a variety of potential applications ranging from chemistry to biological sciences.[1] Metal and semiconductor nanoparticles exhibit interesting size- and shape-dependent properties.[1a,b] Combining these properties with the intrinsic functionalities of organic and biomolecular systems, by incorporating them on the surface of nanoparticles, will yield hybrid materials with novel properties and functions.[1c,d] Using this strategy, the role of gold nanoparticles in modulating the properties of surface-bound fluorophores[1c,2] and their possible applications (for, e.g., electrochemical modulation of fluorescence,[3] light-mediated binding and release of amino acids,[4] and sensitizers for light-harvesting systems[1h]) has been demonstrated. Significant progress has been made in recent years in the development of functional nanomaterials by designing monolayer-protected metal clusters[1k,5−7] and exploiting them as building blocks for supramolecular structures and sensory applications.[1d,8]

Another approach to the design of functional nanomaterials is based on the assembly of biomolecules such as lipids, proteins, and nucleic acids on nanoparticles.[1e,9] Such biomolecular conjugates of nanoparticles can perform specific biomolecular functions and also can be used for the fast and sensitive detection of various biomolecular analytes.[8,10] In most such cases,

(1) (a) Burda, C.; Chen, X.; Narayanan, R.; El-Sayed, M. A. *Chem. Rev.* **2005**, *105*, 1025−1102. (b) Daniel, M.-C.; Astruc, D. *Chem. Rev.* **2004**, *104*, 293−346. (c) Thomas, K. G.; Kamat, P. V. *Acc. Chem. Soc.* **2003**, *36*, 888−898. (d) Shenhar, R.; Rotello, V. M. *Acc. Chem. Res.* **2003**, *36*, 549−561. (e) Niemeyer, C. M. *Angew. Chem., Int. Ed.* **2003**, *42*, 5796−5800. (f) Schmid, G.; Corain, B. *Eur. J. Inorg. Chem.* **2003**, 3081−3098. (g) Adams, D., et al. *J. Phys. Chem. B* **2003**, *107*, 6668−6697. (h) Kamat, P. V. *J. Phys. Chem. B* **2002**, *106*, 7729−7744. (i) Rao, C. N. R.; Kulkarni, G. U.; Thomas, P. J.; Edwards, P. P. *Chem.-Eur. J.* **2002**, *8*, 28−35. (j) Sastry, M.; Rao, M.; Ganesh, K. N. *Acc. Chem. Res.* **2002**, *35*, 847−855. (k) Shipway, A. N.; Katz, E.; Willner, I. *ChemPhysChem* **2000**, *1*, 18−52. (l) Templeton, A. C.; Wuelfing, W. P.; Murray, R. W. *Acc. Chem. Res.* **2000**, *33*, 27−36. (m) Pasquato, L.; Pengo, P.; Scrimin, P. *J. Mater. Chem.* **2004**, *14*, 3481.

(2) (a) Haas, U.; Thalacker, C.; Adams, J.; Fuhrmann, J.; Riethmuller, S.; Beginn, U.; Ziener, U.; Moller, M.; Dobrawa, R.; Wurthner, F. *J. Mater. Chem.* **2003**, *13*, 767−772. (b) Hu, J.; Zhang, J.; Liu, F.; Kittredge, K.; Whitesell, J. K.; Fox, M. A. *J. Am. Chem. Soc.* **2001**, *123*, 1464−1470.

(3) Kamat, P. V.; Barazzouk, S.; Hotchandani, S. *Angew. Chem., Int. Ed.* **2002**, *41*, 2764−2767.

(4) Ipe, B. I.; Mahima, S.; Thomas, K. G. *J. Am. Chem. Soc.* **2003**, *125*, 7174−7175.

(5) Brust, M.; Fink, J.; Bethell, D.; Schiffrin, D. J.; Kiely, C. *J. Chem. Soc., Chem. Commun.* **1995**, 1655−1656.

(6) Jackson, A. M.; Myerson, J. W.; Stellacci, F. *Nat. Mater.* **2004**, *3*, 330−336.

(7) Hostetler, M. J.; Templeton, A. C.; Murray, R. W. *Langmuir* **1998**, *15*, 3782−3789.

(8) (a) Srivastava, S.; Frankamp, B. L.; Rotello, V. M. *Chem. Mater.* **2005**, *17*, 487−490. (b) Verma, A.; Nakade, H.; Simard, J. M.; Rotello, V. M. *J. Am. Chem. Soc.* **2004**, *126*, 10806−10807. (c) Verma, A.; Simard, J. M.; Worrall, J. W. E.; Rotello, V. M. *J. Am. Chem. Soc.* **2004**, *126*, 13987−13991. (d) Hong, R.; Emrick, T.; Rotello, V. M. *J. Am. Chem. Soc.* **2004**, *126*, 13572−13573. (e) Boal, A. K.; Rotello, V. M. *J. Am. Chem. Soc.* **2002**, *124*, 5019−5024. (f) Fischer, N. O.; Verma, A.; Goodman, C. M.; Simard, J. M.; Rotello, V. M. *J. Am. Chem. Soc.* **2003**, *125*, 13387−13391. (g) Shenhar, R.; Jeoung, E.; Srivastava, S.; Norsten, T. B.; Rotello, V. M. *Adv. Mater.* **2005**, *17*, 2206−2210.

(9) Elghanian, R.; Storhoff, J. J.; Mucic, R. C.; Letsinger, R. L.; Mirkin, C. A. *Science* **1997**, *277*, 1078−1081.

(10) Nam, J. M.; Park, S. J.; Mirkin, C. A. *J. Am. Chem. Soc.* **2002**, *124*, 3820−3821.

Scheme 1: Design Strategy for Luminescent Nanomaterials

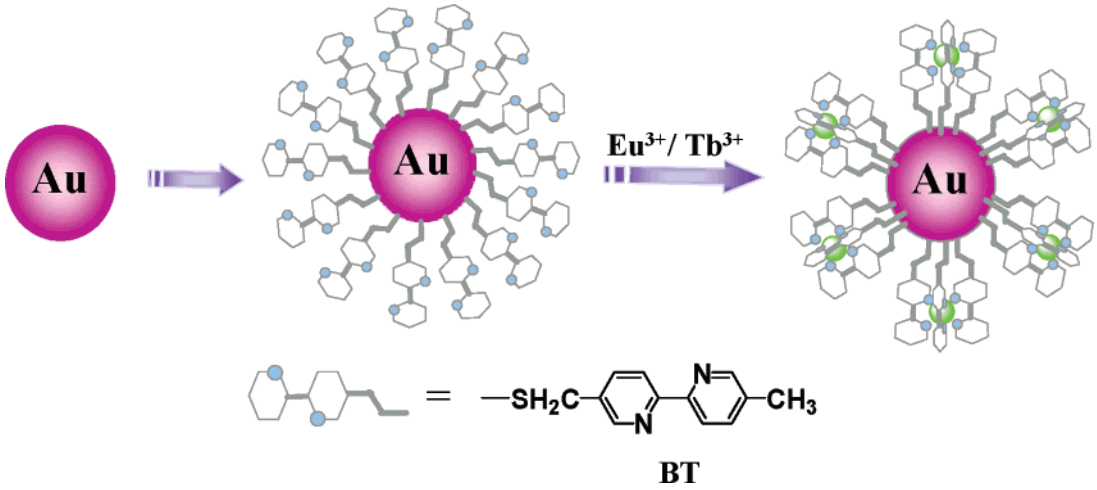

detection is based on the changes in the plasmon absorption band of the Au nanoparticles. Although fluorescence spectroscopy is more versatile and sensitive, it is not often used as a tool for following the properties of metal nanoparticles. This is based on the general belief that the metal nanoparticles strongly quench the singlet excited state of the chromophore when it is attached to their surface. In contrast, recent studies by our group[1c,11a] and others[2a,11b] have shown a dramatic suppression of the quenching of fluorescence when these chromophores are densely packed on the Au nanoparticle surface. This allows the effective utilization of luminescent nanohybrid systems for sensory applications.

Recent studies have shown that Au nanoparticles are rapidly taken up into human cells and that these nanoparticles, with suitable surface modifiers, are nontoxic to human cells.[12a] The biocompatibility of Au nanoparticle conjugates thus allows their potential use for site-specific cellular targeting and nuclear delivery of diagnostic probes and therapeutics.[12b−e] Motivated by these observations, we report here a novel strategy for the design of phosphorescent nanomaterials (Scheme 1) through a bottom-up approach, first by functionalizing a monolayer of 2,2′-bipyridine units on Au nanoparticles (Au−BT) and then further complexing them with lanthanide metal ions such as europium and terbium. Lanthanide complexes with coordinating ligands exhibit long-lived line-like emission[13−17] and are widely used for the detection of biologically important cations and anions,[18−22] as well as organic molecules (for example, phosphoglycerate[23]). More recently, luminescent rare-earth-doped lanthanum phosphate nanoparticles were biofunctionalized with a model protein, namely, avidin, and demonstrated its ability to bind biotin.[24] Use of the newly designed phosphorescent nanomaterial (Au−BT:Eu^{III}) as sensors for biologically important cations is also demonstrated here.

Results and Discussion

Bipyridine-Capped Au Nanoparticles. Bipyridine-capped Au nanoparticles (Au−BT) were synthesized through the sequence of reactions shown in Scheme 2. 5,5′-Dimethyl-2,2′-dipyridyl (**1**) was converted to its monobromo derivative (**2**) using *N*-bromosuccinimide[25] and subsequently to the thiol derivative (BT) using a procedure reported by Fox and coworkers[2b] that involves the reaction of **2** with a mixture of tetrabutylammonium fluoride and hexamethyldisilathiane. The thiol derivative, BT was functionalized onto gold nanoparticles along with 1-dodecanethiol (Au−BT) by following two-phase (water−toluene) reduction of $HAuCl_4$.[26] The presence of alkanethiols was found to be essential for imparting stability to the nanoparticles. The synthesis and characterization of BT and Au−BT are described in the Experimental Section, and the details of the intermediate compounds are available in the Supporting Information.

Absorption spectra of BT and Au−BT in acetonitrile are presented in Figure 1, and TEM images, obtained by drop casting a dilute solution of Au−BT onto a Formvar-coated copper grid, are included in the inset. A stock solution of Au−BT was prepared in toluene from which microliter quantities were injected into acetonitrile (the toluene content in the resultant solution is negligible, <3%). The absorption spectrum of Au−BT (Figure 1B) consists of two bands: the additive

(11) (a) Ipe, B. I.; Thomas, K. G. *J. Phys. Chem. B* **2004**, *108*, 13265−13272. (b) Imahori, H.; Arimura, M.; Hanada, T.; Nishimura, Y.; Yamazaki, I.; Sakata, Y.; Fukuzumi, S. *J. Am. Chem. Soc.* **2001**, *123*, 335−336.
(12) (a) Connor, E. E.; Mwamuka, J.; Gole, A.; Murphy, C. J.; Wyatt, M. D. *Small* **2005**, *1*, 325−327. (b) Tsai, C.-Y.; Shiau, A.-L.; Cheng, P.-C.; Sheih, D.-B.; Chen, D.-H.; Chou, C.-H.; Yeh, C.-S.; Wu, C.-L. *Nano Lett.* **2004**, *4*, 1209−1212. (c) Thomas, M.; Klibanov, A. M. *Proc. Natl. Acad. Sci. U.S.A.* **2003**, *100*, 9138−9143. (d) Tkachenko, A. G.; Xie, H.; Liu, Y.; Coleman, D.; Ryan, J.; Glomm, W. R.; Shipton, M. K.; Franzen, S.; Feldheim, D. L. *Bioconjugate Chem.* **2004**, *15*, 482−490. (e) Hirsch, L. R.; Jackson, J. B.; Lee, A.; Halas, N. J.; West, J. L. *Anal. Chem.* **2003**, *75*, 2377−2381.
(13) Quici, S.; Cavazzini, M.; Marzanni, G.; Accorsi, G.; Armaroli, N.; Ventura, B.; Barigelletti, F. *Inorg. Chem.* **2005**, *44*, 529−537.
(14) Quici, S.; Marzanni, G.; Cavazzini, M.; Anelli, P. L.; Botta, M.; Gianolio, E.; Accorsi, G.; Armaroli, N.; Barigelletti, F. *Inorg. Chem.* **2002**, *41*, 2777−2784.
(15) Sabbatini, N.; Guardigli, M.; Manet, I.; Ungaro, R.; Casnati, A.; Ziessel, R.; Ulrich, G.; Asfari, Z.; Lehn, J.-M. *Pure Appl. Chem.* **1995**, *67*, 135−140.
(16) Sabbatini, N.; Guardigli, M.; Lehn, J.-M. *Coord. Chem. Rev.* **1993**, *123*, 201−228.
(17) Richardson, F. S. *Chem. Rev.* **1982**, *82*, 541−552.
(18) Charbonnie're, L. J.; Ziessel, R.; Montalti, M.; Prodi, L.; Zaccheroni, N.; Boehme, C.; Wipff, G. *J. Am. Chem. Soc.* **2002**, *124*, 7779−7788.
(19) Heck, R.; Dumarcay, F.; Marsura, A. *Chem.-Eur. J.* **2002**, *8*, 2438−2445.
(20) de Silva, A. P.; Fox, D. B.; Huxley, A. J. M.; Moody, T. S. *Coord. Chem. Rev.* **2000**, *205*, 41−57.
(21) Elbanowski, M.; Makowska, B. *J. Photochem. Photobiol. A: Chem.* **1996**, *99*, 85−92.
(22) Faulkner, S.; Mathews, J. L. In *Comprehensive Coordination Chemistry*, 2nd ed.: Ward, M. D., Ed.; Elsevier: Oxford, U.K., 2004; Vol. 9, p 913.
(23) Best, M. D.; Anslyn, E. V. *Chem.-Eur. J.* **2003**, *9*, 51−57.
(24) Meiser, F.; Cortez, C.; Caruso, F. *Angew. Chem., Int. Ed.* **2004**, *43*, 5954−5957.
(25) Ziessel, R.; Hissler, M.; Ulrich, G. *Synthesis* **1998**, 1339−1346.
(26) Brust, M.; Walker, M.; Bethell, D.; Schffrin, D. J.; Whyman, R. *J. Chem. Soc., Chem. Commun.* **1994**, 801−802.

Scheme 2. Reaction Scheme for the Preparation of BT and Au−BT[a]

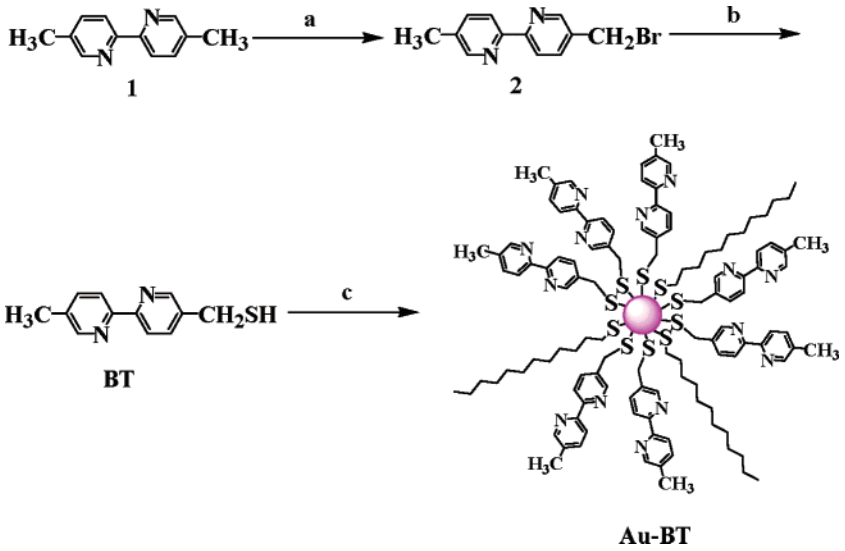

[a] (a) NBS, $CHCl_3$; (b) HMDST, TBAF; (c) 1-dodecanethiol, $HAuCl_4$, TOAB, $NaBH_4$.

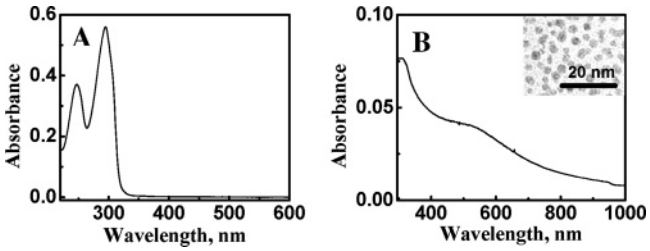

Figure 1. Absorption spectra in acetonitrile of (A) BT and (B) Au−BT. The inset shows the TEM image of Au−BT placed on a Formvar-coated copper grid.

absorption spectrum of BT and gold nanoparticles. The band at 295 nm corresponds to the characteristic $\pi-\pi^*$ transition of bipyridine, which is observed as a shoulder,[16] and the broad band at around 520 nm corresponds to the plasmon absorption of gold nanoparticles. For Au−BT, the short-wavelength band of BT is merged with the absorption of gold nanoparticles.

The TEM image shown in the inset of Figure 1B indicates an average particle size of 4 nm. The functionalization of BT on nanoparticles is not quantitative, and hence, the concentration of unreacted ligands was estimated from the absorbance of BT in the filtrate. Assuming a uniform distribution of BT and dodecanethiol on nanoparticles, the number of BT moieties per nanoparticle is calculated as ∼340, judging from the amount of BT reacted (absorption spectral studies) and the size of the metal core (TEM studies). The above calculation is based on the tight-packed spherical model suggested by Murray and coworkers,[27] according to which gold nanoparticles have a densely packed core of density 58.01 atoms/nm^3 covered with a skin of hexagonally close-packed gold atoms. Thus, each hybrid nanoparticle system consists of a core of ∼820 Au atoms having ∼340 bipyridine ligands, from which the local concentration of BT per nanoparticle is estimated as ∼5 M.

Design and Fabrication of Nanophosphors. Lanthanide ions exhibit long-lived, line-like emission that originates from the radiative transitions of the ^5D_i excited state ($^5D_0$ for the Eu^{III} ion and $^5D_4$ for the Tb^{III} ion) to the various ^7F_j states.[21,28] However, they exhibit low emission yields because of the poor absorption coefficient of ions resulting from the forbidden f−f transition.[16] It is well established that the phosphorescence of lanthanide ions can be enhanced by means of an absorption−energy transfer−emission (A−ET−E) process by encapsulating them in a molecular cavity of coordinating ligands (for example, bipyridine cryptates,[16] phenanthroline derivatives,[13,14] bipyrimidine derivatives[29]). Several factors contribute to the efficiency of luminescence from Eu^{III}/Tb^{III}-ion-based molecular systems: (i) ligand absorption and its ability to shield the ions from their surroundings, (ii) ligand-to-metal ion energy transfer, and (iii) the decay rate constant of metal ion emitting states.[16] The latter aspect is mainly influenced by deactivation due to the presence of solvent molecules that coordinate to the metal ions. Eu^{III}/Tb^{III} complexes containing coordinating solvent molecules such as water exhibit low luminescence yields. This is due to enhanced nonradiative deactivation resulting from the vibronic coupling of the $^5D_0/^5D_4$ excited states with the high-frequency OH oscillators. It is possible to overcome these factors by shielding the lanthanide ions with coordinating ligands that absorb in the UV−vis region and transfer their energy to the lanthanide ions through an energy-transfer process (antenna effect).[13,14,16,29]

One of the significant features of the present nanohybrid system is its high absorption coefficient due to the presence of ∼340 molecules of coordinating bipyridine ligand per Au nanoparticle. In an earlier attempt to increase the absorption efficiency, calix[4]arane[16] and cyclodextrins[19] with varying bipyridine units were synthesized, and it was found that the molar extinction coefficient (ϵ) increases with the number of bipyridine units (the average ϵ value per bipyridine unit for the latter system is estimated as 12500 $M^{-1}cm^{-1}$).[19] The complexation ability of BT/Au−BT with Eu^{III} and Tb^{III} ions was further investigated by following the changes in the absorption spectrum (Figures 2 and 3). The thiol derivative of bipyridine (BT) in acetonitrile exhibits two absorption maxima (Figure 1A): one

(27) Hostetler, M. J., et al. *Langmuir* **1998**, *14*, 17−30.

(28) (a) Werts, M. H. V.; Jukes, R. T. F.; Verhoeven, J. W. *Phys. Chem. Chem. Phys.* **2002**, *4*, 1542−1548. (b) Haas, Y.; Stein, G. *J. Phys. Chem.* **1971**, *75*, 3668−3677.

(29) Shavaleev, N. M.; Accorsi, G.; Virgili, D.; Bell, Z. R.; Lazarides, T.; Calogero, G.; Armaroli, N.; Ward, M. D. *Inorg. Chem.* **2005**, *44*, 61−72.

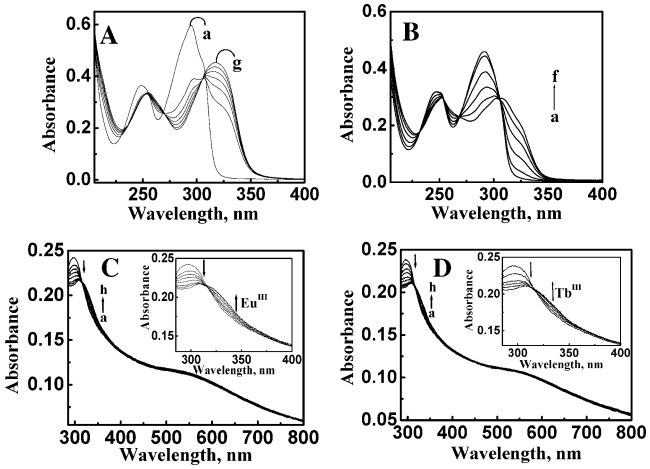

Figure 2. Absorption spectral changes in acetonitrile of (A) BT upon addition of trifluoroacetic acid at (a) 0, (b) 37, (c) 74, (d) 111, (e) 148, (f) 185, and (g) 223 μM; (B) BT upon addition of Eu^{III} ions at (a) 0, (b) 12, (c) 24, (d) 36, (e) 48, and (f) 60 μM; (C) Au−BT upon addition of Eu^{III} ions at (a) 0, (b) 1.1, (c) 2.2, (d) 3.3, (e) 4.4, (f) 5.5, (g) 6.6, (h) and 7.6 μM; and (D) Au−BT upon addition of Tb^{III} ions at (a) 0, (b) 0.6, (c) 1.9, (d) 3.2 (e) 4.5, (f) 5.8, (g) 7.2, and (h) 8.4 μM.

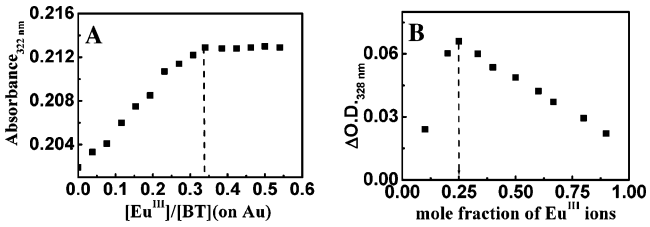

Figure 3. (A) Plot of the absorbance at 322 nm as a function of Eu^{III}/BT mole ratio (BT bound on Au nanoparticles). (B) Job's plot obtained for a 1:3 complexation between Eu^{III} ions and BT bound on Au nanoparticles.

at 249 nm and the other at 295 nm. Upon addition of increasing concentrations of Eu^{III} ions, a decrease in the intensity of the $\pi-\pi^*$ absorption band (295 nm) of BT along with the concomitant emergence of a new band around 325 nm (Figure 2B) was observed. Similar spectral changes were observed for BT upon addition of acid (Figure 2A), and the monoprotonation results in a conformational change to the cis form. The emergence of a new band for BT/Au−BT at 325 nm upon addition of Eu^{III}/Tb^{III} ions is attributed to the polarization resulting from the metal ion coordination and the conformation change of the ligand to the cis form (Figure 2C,D).

The stoichiometry for the complexation of Eu^{III}/Tb^{III} ions with Au−BT was investigated by means of the absorption isotherm[30a] and Job's continuous variation method[30b] (Figure 3). After successive additions of Eu^{III} ions, solutions were kept for equilibration (~30 min), and the changes in absorbance were monitored. The increase in absorbance at 322 nm, when plotted against the mole ratios of metal ions to BT (bound to Au nanoparticles), reached a saturation point at 0.33, indicating a 1:3 metal ion-to-ligand stoichiometry (Figure 3A and Supporting Information). To further confirm the stoichiometry, difference absorption spectra were recorded by varying the mole ratio of BT bound on Au nanoparticles to Eu^{III}/Tb^{III} ions (Supporting Information). The difference absorption spectra highlight the spectral differences resulting from the varying concentrations

(30) (a) Folmer-Andersen, J. F.; Lynch, V. M.; Anslyn, E. V. *Chem. Eur. J.* **2005**, *11*, 5319−5326. (b) Connors, K. A. *Binding Constants: The Measurements of Molecular Complex Stability*; Wiley: New York, 1987.

Chart 1. Two Possible Modes of Complexation between Eu^{III}/Tb^{III} Ions and Bipyridines Bound on Au Nanoparticles

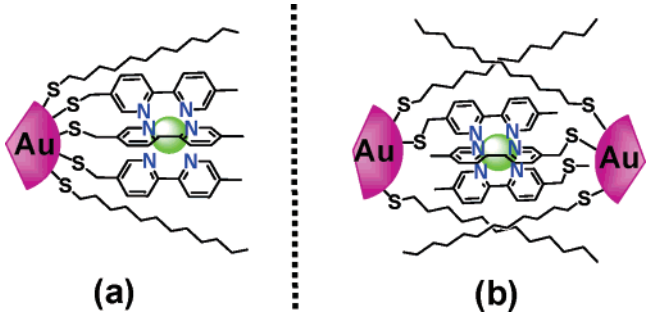

of complexed and uncomplexed bipyridines on gold nanoparticles. The corresponding Job's plot showed a maximum value for the absorbance at 328 nm when the mole fraction of Eu^{III}/Tb^{III} ions reached 0.25, indicating a 1:3 binding between metal ions and bipyridines bound on Au nanoparticles (Figure 3B and Supporting Information).

A 1:3 complexation stoichiometry between metal ions and BT bound on Au nanoparticles allows two major modes of interactions (Chart 1): (a) bipyridines bound on the same Au nanoparticle coordinating with Eu^{III}/Tb^{III} ions and (b) bipyridines from different nanoparticles coordinating to a given lanthanide ion. To investigate these aspects, the TEM images of the Au−BT complexes were recorded in the absence (inset of Figure 1B) and the presence of Eu^{III} ions (Figure 4), under otherwise identical conditions (by drop casting the solution used for spectroscopic investigation onto a Formvar-coated copper grid). Bipyridine-capped Au nanoparticles are randomly distributed through out the grid (Figure 1B), whereas self-assembly is observed in the presence of Eu^{III} ions (Figure 4). The tendency toward aggregation observed in absorption spectral studies and self-assembled structures in the TEM images support the later possibility (Chart 1b).

Luminescence Efficiency of Nanophosphors. The luminescence properties of Au−BT complexes containing varying concentrations of Eu^{III}/Tb^{III} ions were investigated by using steady-state and time-resolved techniques. In the case of Au−BT, a weak unstructured emission band was observed between 320 and 450 nm that is characteristic of bipyridine fluorescence (Supporting Information). A dramatic enhancement of the emission intensity was observed upon addition of varying concentrations of Eu^{III}/Tb^{III} ions (excitation at 320 nm), and the luminescence intensity leveled off at higher concentrations (Figure 5). The Au−BT:Eu^{III} complex features six line-like emission peaks at 578, 594, 619, 649, 693, and 702 nm, whereas the Au−BT:Tb^{III} complex exhibits four major line-like emission peaks at 487, 546, 584, and 640 nm. The enhancement in line-like emission is attributed to the complex's ability to effectively shield the encapsulated metal ion and efficient energy-transfer process from the BT molecules to the coordinated Eu^{III}/Tb^{III}

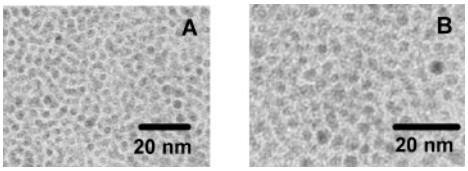

Figure 4. TEM image of Au−BT in the presence of Eu^{III} at two different magnifications.

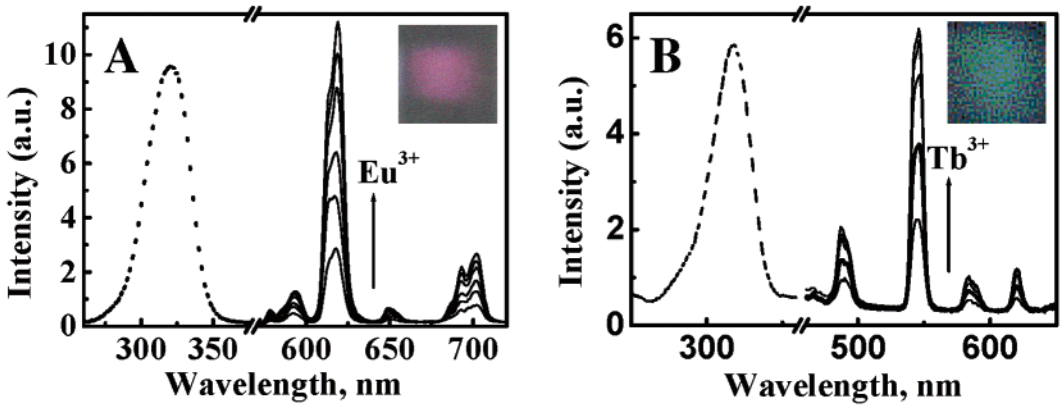

Figure 5. Luminescence spectrum of Au−BT in acetonitrile (A) upon addition of Eu^{III} at (a) 2.4, (b) 4.8, (c) 7.2, (d) 9.7, (e) 12, and (f) 14.5 μM and (B) upon addition of Tb^{III} at (a) 5.5, (b) 11, (c) 16.6, (d) 22, and (e) 27.7 μM after excitation at 320 nm. The dotted line shows the excitation spectrum of the complex in acetonitrile (A) at 14.5 μM Eu^{III} (emission followed at 616 nm) and (B) at 27.7 μM Tb^{III} (emission followed at 545 nm). The inset shows a photograph of a cuvette containing acetonitrile solution of Au−BT:Eu^{III} and Au−BT:Tb^{III} complexes illuminated using a 320-nm UV light source.

ions. The insets of Figure 5A,B show photographs of cuvettes containing acetonitrile solutions of red-emitting Au−BT:Eu^{III} and green-emitting Au−BT:Tb^{III} complexes illuminated using a 320-nm UV light source.

The luminescence quantum yields (ϕ) were found to be 9.6×10^{-3} and 38.0×10^{-3} for the Au−BT:Eu^{III} and Au−BT:Tb^{III} complexes, respectively (measured for the 1:3 metal ion-to-ligand complex). The quantum yields obtained by the method described by Haas and Stein[28b] using $Ru[(bpy)_3]^{2+}$ ($\phi = 0.028$ in aerated water)[31] as a standard for the Au−BT:Eu^{III} complex and quinine sulfate ($\phi = 0.546$ in 1 N H_2SO_4)[33] for the Au−BT:Tb^{III} complex. The luminescence quantum yields of Au−BT:Eu^{III}/Tb^{III} complexes are higher than those of Eu^{III}/Tb^{III} complexes of cryptands and calixarenes containing bipyridine units.[16] The origin of the luminescence was further investigated by recording the excitation spectra (dotted lines in Figure 5) of Au−BT:Eu^{III} and Au−BT:Tb^{III} complexes, following the emission at 616 and 545 nm, respectively. In both cases, the excitation spectrum peaks at 320 nm, indicating that the ligand-centered excited state populates the emitting levels of Eu^{III}/Tb^{III} ions through an energy-transfer process, resulting in emission from the $^5D_i-^7F_j$ states.

Lanthanide complexes are widely used as fluoroimmunoassay labels by taking advantage of their long-lived emission (lifetimes are in the millisecond range).[16,21,32] The autofluorescence of biological materials usually decays on the nanosecond time scale, which overlaps with the lifetime of organic fluorophores, limiting their application as fluorescent labels in biological systems. In contrast, luminescent lanthanide complexes have the obvious advantage of eliminating the background emission from a biological matrix. Interestingly, the luminescence lifetimes of lanthanide complexes are not influenced by linking them onto gold nanoparticles. The room-temperature phosphorescence lifetimes of the Au−BT:Eu^{III} and Au−BT:Tb^{III} complexes (τ measured for 1:3 metal ion-to-ligand complex) were estimated as 0.36 and 0.7 ms, respectively.[34] The solutions were thoroughly degassed before the lifetime studies were conducted, and the plots of the luminescence decay for

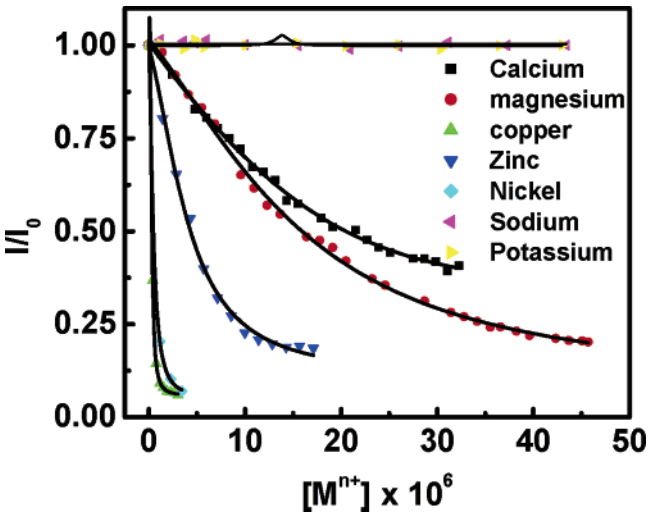

Figure 6. Relative decrease in the luminescence intensity of Au−BT-Eu^{III} in the presence of various concentrations of different metal ions.

Au−BT:Eu^{III} and Au−BT:Tb^{III} complexes are presented in the Supporting Information.

Sensor Performance. One of the significant features of the Au−BT:Eu^{III}/Tb^{III} system is its ability to hold a large number of lanthanide complexes around the Au nanoparticle without affecting their luminescence behavior (long-lived line-like emission). Such nanophosphors are ideal as high-affinity sensors for the site-specific detection of biologically important cations. It is well established that a proper balance in the concentrations of various metal ions such as Ca^{2+} and Mg^{2+} is vital in performing various biological functions. For example, intracellular Ca^{2+} regulates the contraction of cardiac and smooth muscles.[35] However, their determination in complex biological systems is rather difficult because they are present in specific locations with a concentration gradient (calcium channels).

(31) Nakamura, K. *Bull. Chem. Soc. Jpn.* **1982**, *55*, 2697.
(32) Werts, M. H. V.; Woudenberg, R. H.; Emmerink, P. G.; van Gassel, R.; Hofatraat, J. W.; Verhoeven, J. W. *Angew. Chem., Int. Ed.* **2000**, *39*, 4542−4544.
(33) Meech, S. R.; Philips, D. *J. Photochem.* **1983**, *23*, 193.
(34) Phosphorescence lifetimes were measured in a SPEX model 1934D phosphorimeter equipped with a flash lamp. The signals from the sample falling on the photomultiplier were collected by a control module for a preset length of time. The luminescence intensities decay exponentially with first-order kinetics over time t, obeying the equation $I_t = I_0 \exp(-t/\tau)$, where I_0 and I_t are the luminescence intensities at time zero and time t, respectively. The emission lifetime was obtained by fitting the decay curve to the above equation.
(35) Voet, D.; Voet, J. G. *Biochemistry*, 2nd ed.; John Wiley & Sons: New York, 1995.

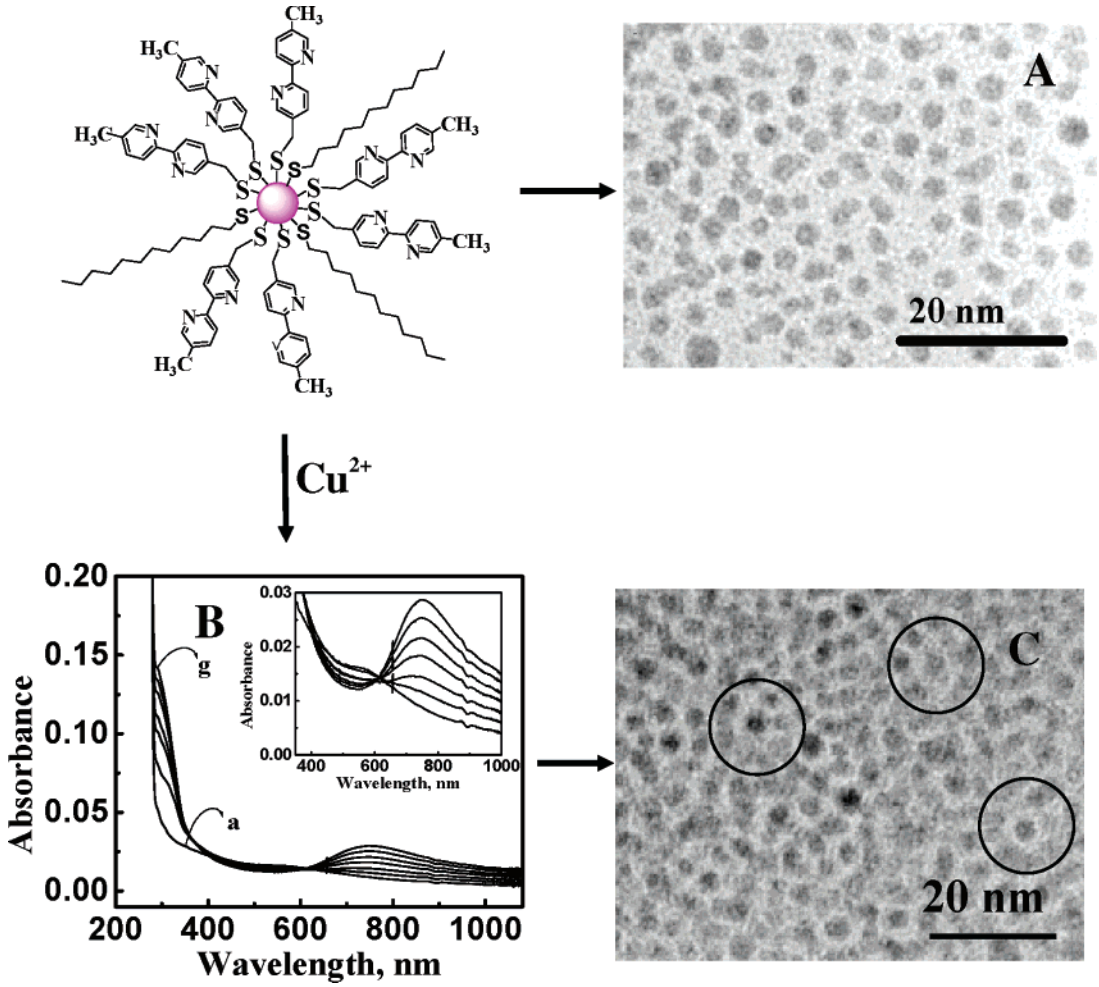

Figure 7. (A) TEM image and (B) absorption spectra of Au−BT upon addition of [Cu^{2+}] at (a) 0, (b) 32, (c) 63, (d) 95, (e) 127, (f) 158, and (g) 190 μM. (C) TEM image of Au−BT in the presence of Cu^{2+}.

Isomorphous replacement of metal cations (for example, Ca^{2+}) by Eu^{III}/Tb^{III} ions has been widely used for sensing applications.[21] Substitution of Eu^{III}/Tb^{III} ions by various metal cations mainly depends on the similarity in size of the cation and its binding ability.[21] The ability of the luminescent Au−BT:Eu^{III} complex to sense alkali metal ions (Na^+, K^+), alkaline earth metal ions (Ca^{2+}, Mg^{2+}), and transition metal ions (Cu^{2+}, Ni^{2+}, Zn^{2+}) was investigated. The relative decreases in the luminescence intensities of an acetonitrile solution of the Au−BT:Eu^{III} complex in the presence of various metal ions are represented in Figure 6. It can be noted that, upon addition of various metal cations, no noticeable absorption spectral changes were observed (Supporting Information).

A dramatic decrease in the luminescence was observed upon addition of alkaline earth metal ions and transition metal ions, whereas the luminescence intensity was not influenced by the addition of Na^+ and K^+ ions (after successive additions, the solution was allowed to stand for 5 min, for attaining equilibrium, in each case). The relative decrease in intensity is much larger for transition metal ions as compared to alkaline earth metals. This might be due to the better binding ability of the transition metal ions over Eu^{III} ions.

Superstructure Formation of Au−BT. Transition metal ions form stable complexes with various coordinating ligands such as bipyridine[36] and phenanthroline.[37] The formation of superstructures and cross-linked nanoparticle stripes through the interaction of terpyridine-functionalized Au nanoparticles and metal salts has been reported recently.[8g] The direct interaction of Au−BT with Cu^{2+} ions was investigated by following the absorption spectral changes (Figure 7). Upon the addition of an acetonitrile solution of Cu^{2+} to Au−BT, we observe (i) the formation of a new band at 310 nm that is merged with the Au nanoparticle absorption and (ii) the emergence of red-shifted band at 780 nm, along with a concomitant decrease in the plasmon absorption band of Au−BT at 520 nm (inset of Figure 7B).

The band at 780 nm is not observed in the case of BT upon addition of Cu^{2+} ions. The absorption band in the short-wavelength region (310 nm) results from the conformation change of the ligand to the cis form and the complexation of Cu^{2+} ions with bipyridines. Attempts to determine the stoichiometry of complexation between BT on Au nanoparticles and Cu^{2+} ions using Job's continuous variation method were not successful because of the strong aggregation tendency of the nanoparticles in the presence of copper ions. Analysis of TEM images of Au−BT in the absence and presence of Cu^{2+} clearly indicates the formation of superstructures upon metal ion complexation. The strong coordinating ability of Cu^{2+} ions can bring the Au−BT nanohybrids together, leading to the formation of superstructures. The images presented in the highlighted

(36) Kaes, C.; Katz, A.; Hosseini, M. W. *Chem. Rev.* **2000**, *100*, 3553−3590.
(37) Armaroli, N. *Chem. Soc. Rev.* **2001**, *30*, 113−124.

portion of Figure 7C show ring structures with an external diameter of about 10 nm.

The absorption band at 780 nm originates from interparticle plasmon coupling because of the close interaction of metal nanoparticles in these superstructures. When electromagnetic radiation interacts with Au nanoparticles, its electric vector displaces the electron cloud, which is restored by the Coulombic attraction of the nucleus, and this establishes the oscillation of plasmon electrons. Surface plasmon absorption originates when this frequency of oscillation is in resonance with that of incident radiation. When two or more metal nanoparticles are placed in close proximity, an additional force of attraction between the electron cloud and nucleus of adjacent nanoparticles becomes significant. A decrease in the frequency of plasmon oscillation was observed because of the perturbed charge distribution of assembled Au nanoparticles. This results in the formation of the red-shifted band at 780 nm and a concomitant decrease in the plasmon absorption band of Au−BT at 520 nm. Such interparticle plasmon interactions were observed in Au superstructures,[1d,i,k] closed-loop structures of Au nanoparticles (nanonecklaces),[38] closely spaced Au nanoparticles deposited on ITO glass plates,[39] and longitudinally organized Au nanorods.[40]

Conclusions

The chelating agent 2,2′-bipyridine was anchored to Au nanoparticles, and their complexation with Eu^{III}/Tb^{III} ions yielded red-emitting Au−BT:Eu^{III} and green-emitting Au−BT:Tb^{III} phosphorescent nanomaterials (nanophosphors). The ligand-centered excited state of the complex populates the emitting levels of Eu^{III}/Tb^{III} ions through an energy-transfer process, resulting in the emission from the $^5D_0/^5D_4-^7F_j$ levels. A 1:3 complexation stoichiometry was observed between Eu^{III}/Tb^{III} ions and BT bound on Au nanoparticles, and the self-assembled structures observed in TEM images indicate the possibility of a given lanthanide ion coordinating with bipyridines from different nanoparticles. An attractive feature of the present systems is their ability to hold a large number of luminescent lanthanide complexes around Au nanoparticles without affecting the long-lived line-like emission properties. Such phosphorescent nanohybrid systems might have wide range of applications in optoelectronic devices and biomolecular systems. In the present case, we have used them as high-affinity sensors for the selective detection of cations through isomorphous substitution of lanthanide ions. Because gold nanoparticles can be easily functionalized with molecules that can selectively bind at specific sites, such phosphorescent nanomaterials can be used in understanding the properties and functions of various biological processes and in determining biologically active substances.

Experimental Section

Details of instrumental methods for spectroscopic characterization are presented in the Supporting Information. Stock solutions of the lanthanides were prepared by dissolving europium(III) chloride and terbium(III) chloride in methanol, and microliter quantities were added to the Au−BT solution. The monobromo derivative of 5,5′-dimethyl-2,2′-dipyridyl (**2**) was prepared as per a reported procedure[25] (Supporting Information). Conversion of **2** to the thiol derivative (BT) and its functionalization on gold nanoparticles are described below. Freshly distilled solvents were used throughout.

Synthesis of Compound BT. To an ice-cooled solution of compound **2** (200 mg, 0.76 mmol) in THF (3 mL) was added a mixture of tetrabutylammonium fluoride (221 mg, 0.84 mmol) and hexamethyldisilathiane (166.8 mg, 0.92 mmol) in THF (2 mL) under stirring. The reaction mixture was stirred for a further period of 12 h. It was then diluted with dichloromethane and washed with saturated ammonium chloride (10 mL) and then with distilled water (20 mL × 2). The organic layer was separated and dried over anhydrous sodium sulfate, and the solvent was removed under reduced pressure to give a residue that was recrystallized from a mixture (9:1) of hexane and ethyl acetate to yield white crystals of BT (40 mg, 40%), mp 106 °C. IR (KBr) ν_{max}: 2369, 1593, 1560, 1465, 1371, 1236, 1128, 1027, 838, 737, 663 cm^{-1}. ^1H NMR ($CDCl_3$, 300 MHz) δ (ppm): 2.39 (s, 3H, $-CH_3$), 3.66 (s, 2H, $-CH_2SH$), 8.51 (s, 1H, ar), 8.49 (s, 1H, ar), 8.34−8.31 (d, 1H, J = 8.1 Hz, ar), 8.28−8.26 (d, 1H, J = 8.1 Hz, ar), 7.70−7.68 (d, 1H, J = 8.1 Hz, ar), 7.69−7.67 (d, 1H, J = 8.1 Hz, ar). ^{13}C NMR ($CDCl_3$, 75 MHz) δ (ppm): 32.57, 40.06, 120.6, 132.65, 137.5, 149.6, 153.16, 155.46. Exact mass calcd. for $C_{12}H_{12}N_2S$ [MH^+]: 217.0799, found 217.0805 (FAB, high-resolution mass spectroscopy).

Synthesis of Gold Nanoparticles Capped with BT. To a stirred solution of tetraoctylammonium bromide (0.068 g,) in toluene (5 mL) was added dropwise an aqueous solution of hydrogentetrachloroaurate-(III) hydrate (11 mg, 0.028 mmol), and the mixture was stirred for 20 min. The reaction mixture was washed with distilled water (10 mL) several times, and the organic layer was separated. A mixture of BT (4.2 mg, 0.0196 mmol) and dodecanethiol (1.7 mg, 0.0084 mmol) in toluene (2 mL) was added to the above solution, and the resulting mixture was stirred for 30 min. An aqueous solution of sodium borohydride (11 mg, 0.28 mmol) was added dropwise, and the mixture was stirred for a further period of 3 h. The organic layer was washed with water and diluted with methanol (250 mL). It was kept in a refrigerator, and the precipitate obtained was further purified by being resuspended in toluene and then centrifuged after the addition of methanol (10 mL). This process was repeated twice to remove any unbound thiol. The residue obtained was redispersed in 5 mL of toluene and used as stock solution.

Acknowledgment. The authors thank the Council of Scientific and Industrial Research (CMM 220239), and the Department of Science and Technology (SP/S5/NM-75/2002), Government of India, for financial support. We thank Prof. C. N. R. Rao for use of HRTEM facilities at the Jawaharlal Nehru Centre for Advanced Scientific Research, Bangalore, India. This is contribution no. RRLT-PPD-200 from the Regional Research Laboratory, Trivandrum, India.

Supporting Information Available: Details on the preparation, purification, and characterization of **2**; difference absorption spectra of Au−BT in the presence of Eu^{III}/Tb^{III} ions; absorption isotherm and Job's plot for a 1:3 complexation between Tb^{III} ions and BT bound on Au nanoparticles; lifetime studies of Au−BT:Eu^{III} and Au−BT:Tb^{III} complexes; and complete refs 1g and 27. This material is available free of charge via the Internet at http://pubs.acs.org.

JA054347J

(38) Dai, Q.; Worden, J. G.; Trullinger, J.; Huo, Q. *J. Am. Chem. Soc.* **2005**, *127*, 8008−8009.
(39) Rechberger, W.; Hohenau, A.; Leitner, A.; Krenn, J. R.; Lamprecht, B.; Aussenegg, F. R. *Opt. Commun.* **2003**, *220*, 137−141.
(40) (a) Thomas, K. G.; Barazzouk, S.; Ipe, B. I.; Joseph, S. T. S.; Kamat, P. V. *J. Phys. Chem. B* **2004**, *108*, 13066−13068. (b) Sudeep, P. K.; Joseph, S. T. S.; Thomas, K. G. *J. Am. Chem. Soc.* **2005**, *127*, 6516−6517.